CCD IMAGERY, *uvbyβ* PHOTOMETRY, AND THE PHYSICAL PARAMETERS OF HAFFNER 19[1]

M. A. Moreno-Corral, C. Chavarría-K, and E. de Lara

Instituto de Astronomía
Universidad Nacional Autónoma de México, Ensenada, B. C., México

RESUMEN

Se presenta fotometría $UBV(RI)_c$ de 334 estrellas del cúmulo Haffner 19 que complementa y amplía la existente, extendiéndola hasta la magnitud $m_\lambda = 19$ ($\lambda = U, B, V, R, I$). Usando los diagramas $(V, B-V)$, $(V, V-I)$, $(I, R-I)$, $(U-B, B-V)$ y $(V-R, V-I)$ resultantes, se establece la pertenencia de 102 estrellas, triplicando la información hasta ahora publicada. Esa fotometría permitió clasificar espectralmente 33 estrellas, confirmando la juventud de 29 (15 B0–B1 y 14 B2–B9). Para confirmar independientemente la distancia y enrojecimiento del cúmulo, se hizo fotometría fotoeléctrica $uvbyβ$ de 6 estrellas brillantes. Se estudia imágenes CCD de banda angosta en Hα, [N II] y [S II], que revelan la presencia de una esfera de Strömgren en el cúmulo. Nuestros datos fotométricos, analizados usando 4 métodos diferentes, indican enrojecimiento homogéneo $E_{B-V} = 0.42 \pm 0.01$ para Haffner 19, además permiten establecer una distancia de 5.2 ± 0.4 kpc, y restringen el intervalo de edad entre 10^6 y 3.7×10^6 a, con 2×10^6 a como el valor más probable, lo que no permite deducir en forma confiable su metalicidad. Finalmente se presentan por separado las velocidades radiales de Haffner 18ab, Haffner 19 y NGC 2467, las que indican que los dos últimos se hallan a la misma distancia.

ABSTRACT

We present broad-band $UBV(RI)_c$ CCD imagery of 334 stars in the direction of the Galactic cluster Haffner 19. The sample is complete to $m_\lambda = 19$ ($\lambda = U, B, V, R, I$). We reliably establish the cluster membership for 102 stars based upon their locations in the $(V, B-V)$, $(V, V-I)$, $(I, R-I)$, $(U-B, B-V)$, and $(V-R, V-I)$ diagrams, thus increasing three-fold the number of known cluster members. With the Q-method we determine the MK spectral types of the 33 brightest stars, confirming that 29 belong to the cluster's young population (15 B0–B1 and 14 B2–B9 main sequence stars). Complementary $uvbyβ$ photoelectric photometry of 6 bright stars independently confirms the distance and reddening to the cluster. Our narrow-band Hα, [N II], and [S II] imagery reveals the presence of a Strömgren sphere and we derive its properties. From our photometric data and by four different means we find that the best distance estimate to the cluster is 5.2 ± 0.4 kpc, with a fairly homogeneous reddening of $E_{B-V} = 0.42 \pm 0.01$. The data constrain the age of the cluster to be between 10^6 and $\leq 3.7 \times 10^6$ years, with 2×10^6 yr as its most likely estimate. Because of its young age, it is not possible to derive a reliable estimate for its metallicity. Finally, we present radial velocities of Haffner 18ab, Haffner 19, and NGC 2467, which place the last two of these at the same distance.

Key Words: **H II REGIONS — OPEN CLUSTERS AND ASSOCIATIONS, INDIVIDUAL: HAFFNER 19, HAFFNER 18AB, NGC 2467 — TECHNIQUES: PHOTOMETRIC**

---

1. INTRODUCTION

Haffner 19 is a Galactic cluster of spherical form, located in the direction of Puppis ($\ell = 243°1$, $b = 0°5$), originally reported by Haffner (1957), who found that it consisted of at least 14 stars brighter than $m_{\mathrm{pg}} = 16.5$, and estimated its apparent diameter to be $\phi = 1'8$. Lodén (1965) reported a spectral type B1.5V for the brightest star CD-$25°5202$ in its center, determined by W. W. Morgan, and measured it photoelectrically ($V = 11.09$, $B-V = +0.26$ and $U-B = -0.53$). Later, FitzGerald & Moffat (1974, FM74 hereafter) established from the stellar density the existence and size of the cluster (FWHM $= 1.2'$) and also reported photoelectric and photographic UBV photometry of 39 stars brighter than $V = 16.0$. Of these, 23 ± 7 should belong to Haffner 19. They also observed CD-$25°5202$ spectroscopically, determining its MK spectral type to be B0V, i.e., hotter than that reported previously by Lodén (1965). In a complementary report based upon new data, FitzGerald & Moffat (1976) revised their previous work on the region, obtaining basically their earlier results and conclusions. Pişmiş & Moreno (1976, PM76 herein) give a kinematic distance estimate to NGC 2467 and report an Hα shell surrounding CD$-25°5202$. More recently, Labhardt, Spaenhauer, & Schwengeler (1992, LSS92 herafter) and Munari & Carraro (1996, MC96 from now on) presented CCD broad-band photometry of Haffner 19 ($BVGR$ and $UBV(RI)_c$, respectively) and estimated the reddening and distance to the region. MC96 also determined spectroscopically the MK spectral types of four bright stars associated with the cluster.

Although the photometric systems and methods employed supposedly are the same (e.g., Johnson's UBV), the distances obtained by different authors disagree significantly by more than the uncertainties in the observations involved. Much of this is due to the different photometric (secondary) reference systems and their calibration (cf. Moro & Munari 2000). Another problem is that the photometric distances differ from those estimated kinematically. In addition, Haffner 19, Haffner 18ab, and NGC 2467 may not be physically associated, but they have been observed in the past as a single entity. Different approaches to the regions are now found in the literature (e.g., LSS92, MC96; Moitinho 2000, 2001), but important discrepancies remain. Because of this, we decided to complement the work of MC96 and extend the $UBV(RI)_c$ photometry of the stellar content in the central part of Haffner 19 to $m_\lambda \geq 19$ ($\lambda = U, B, V, R, I$), reanalyzing the stellar member-
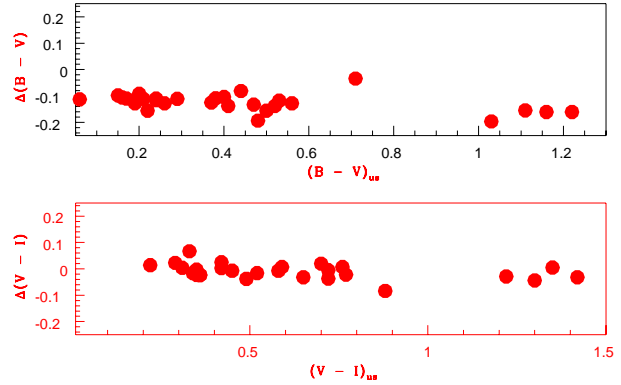
Fig. 1. Comparison of the color differences $(B-V)$ and $(V-I)$ between this paper (us) and MC96 as a function of the color indices $(B-V)_{\mathrm{us}}$ and $(V-I)_{\mathrm{us}}$ are displayed in the upper and lower panel, respectively.

ship, reddening, distance and age of the cluster. In order to complement, at least partially, the scarce information regarding the ionized gas of the region (to our knowledge there is little or nothing at radio wavelengths), we have obtained narrow-band CCD imagery of the cluster in the Hα, [N II], and [S II] lines. In addition, we have revised earlier Fabry-Perot interferograms of the region by PM76, reducing separately Haffner 19, Haffner 18ab, and NGC 2467. The stellar photometric data are complete down to a magnitude $m_\lambda = 19$ ($\lambda = U, B, V, R, I$) within the field of view of the CCD chip ($\approx 3.9 \times 3.9$ arcmin^2). For the first time, we report $uvby\beta$ photoelectric photometry of 6 stars in the field of the cluster, which allows us to determine, independently of previous calibrations reported elsewhere, their spectral types, reddening and membership of the cluster, and to estimate a color excess and a distance to the stellar aggregate. Additionally, based upon narrow band Hα, [N II], and [S II] imagery we discuss the ionization structure of the Strömgren sphere surrounding CD$-25°5202$. In the following, we present our data and discuss our results.

2. OBSERVATIONS AND DATA REDUCTION

2.1. *CCD Imagery and $UBV(RI)_c$ Photometry*

$UBV(RI)_c$, Hα, [N II] $\lambda6584$ Å and [S II] $\lambda6731$ Å imagery of Haffner 19 was carried out on 1996 December 6 with a direct camera equipped with a cooled ($-100°C$) Thomson 1024×1024 pixel^2 (pixel size $= 19$ μm) CCD detector coated with a Metachrome II film, with a dark current of 0.31 e$^-$/(pixel-sec) at gain 4 ($= 2.7$ e$^-$/ADU) and a readout noise of 3.47 e$^-$. Its linearity is 0.58%. The camera was attached to the Cassegrain focus of the 1.5 m "Harold L. Johnson" telescope of Sierra

San Pedro Mártir National Astronomical Observatory (SPMO). The telescope was masked to 1.3 m (f/13.05) in order to obtain better images. The exposure times for the $BV(RI)_c$ filters were of 90 s each and for the U filter was 180 s. For the narrow-band filters the exposures were of 180 s each. The plate scale was of 0.231 arcsec/pixel. The FWHM diameter of the stars on the guided images is $\leq$ 1.4 ± 0.1 arcsec for all 7 filters discussed here. The night was photometric.

TABLE 1

$UBV(RI)_c$ PHOTOMETRY OF HAFFNER 19

Nr.	Others	(X, Y)	V	$B-V$	$U-B$	$V-R$	$V-I$	Member	SpT(Q)	Remarks
1		$(834.65, 872.48)$	19.35	2.47		0.79	1.60	nm		
1a		$(855.92, 856.02)$	18.63	1.13		0.57	1.20	nm?		
1b		$(860.84, 905.79)$	17.50				1.21			
2		$(597.87, 882.71)$	16.61	0.88	0.52	0.71	1.22	nm		U, B:
2a		$(637.82, 900.24)$								$R = 19.5$
3		$(342.06, 894.27)$	17.95	1.50		0.61	1.41	nm		
3a		$(331.42, 869.66)$	18.82	1.63		0.59	1.09	nm		
3b		$(352.71, 863.69)$	18.36	1.21		0.47	1.20	nm		
4		$(286.48, 877.46)$	14.87	0.64	0.30	0.38	0.77	nm		
5		$(167.83, 867.97)$	16.23	0.98	0.09	0.55	1.14	nm		
6		$(119.54, 849.94)$	16.16	0.64	0.27	0.38	0.82	m		
6a		$(121.52, 829.18)$	15.60	1.04	0.21	0.55	1.07	nm		U, B:
7		$(143.03, 849.74)$	17.64	0.74	-0.11	0.50	1.14	m		
8		$(494.91, 894.06)$	17.50				-0.36			
8a		$(494.07, 876.74)$	16.70	1.38		0.49	0.01	nm		
8b		$(474.01, 855.90)$	19.05	1.53	-2.17	0.39	1.31	nm		
9	LSS48	$(594.36, 849.49)$	15.19	0.64	0.00	0.46	1.03	nm		
10	LSS47	$(651.67, 844.44)$	15.62	0.60	0.08	0.39	0.78	nm		
10a		$(647.32, 862.62)$	20.67	2.31		1.04	2.12	nm		B:
11		$(744.30, 874.32)$	18.36	1.00		0.52	1.04	m		
12		$(790.08, 859.13)$	17.93	1.23		0.63	1.26	m		
13		$(620.67, 828.60)$	17.23	0.87	-0.17	0.43	0.92	nm?		
14		$(489.33, 828.50)$	17.09	0.74		0.46	0.93	m		
14a		$(486.92, 821.94)$	19.17	0.95			1.78	m		
14b		$(526.45, 806.45)$	18.49	1.14			1.15	nm		
15		$(865.54, 796.62)$	17.12	0.74		0.44	0.90	m		
15a		$(831.00, 804.15)$								$R = 19.0$:
16		$(755.73, 805.06)$	18.20	1.57		0.71	1.37	nm		
16a		$(775.70, 828.45)$								$R = 19.1$:
17		$(738.25, 797.37)$	17.50	1.02		0.51	1.05	nm		
18	FM4021	$(553.13, 787.72)$	15.76	1.02	0.72	0.61	1.23	nm		U:
18a		$(581.65, 763.54)$	20.13	1.22		0.91	1.97	m		B:
19		$(259.30, 810.37)$	18.08	1.22		0.53	1.04	nm		
19a		$(302.34, 818.70)$	19.1:			0.73	1.52	m		
19b		$(307.67, 796.71)$								$R = 18.7$:
20	FM3120	$(202.96, 788.32)$	13.30	1.14	0.92	0.63	1.24	nm		

TABLE 1 (CONTINUED)

Nr.	Others	(X, Y)	V	$B-V$	$U-B$	$V-R$	$V-I$	Member	SpT(Q)	Remarks
20a		$(223.10, 802.05)$	19.61	2.38				nm		B:
21		$(245.13, 779.47)$	17.45	0.93		0.43	0.87	nm		
22		$(255.30, 777.46)$	18.11	1.18		0.49	0.92	nm		
23	FM4022	$(501.63, 771.56)$	14.99	0.29	-0.24	0.20	0.47	m	B3V	
24		$(761.39, 779.06)$	16.20	0.81	0.16	0.45	0.97	nm		
24b		$(783.12, 777.51)$	19.11	2.76		0.35	0.72	nm		
25		$(814.68, 766.20)$	17.59	0.96	-0.73	0.50	0.02	nm		
26	LSS44	$(667.90, 763.05)$	16.40	0.63	-4.63	0.38	0.83	m		U:
27		$(669.14, 749.52)$	18.74	1.21	-1.22	0.75	1.42	nm		U, B:
28	LSS43	$(645.61, 757.84)$	16.51	0.41	0.29	0.31	0.69	m		
28a		$(621.79, 768.58)$	19.83	5.44		0.62	1.34	nm?		B, V::
29	LSS42	$(606.47, 746.43)$	16.71	0.90	-0.06	0.47	0.95	nm		B, V:
30		$(542.58, 734.97)$	19.03	2.82		0.59	1.25	nm		B, V:
31		$(496.95, 755.02)$	18.26	1.03	-0.43	0.51	1.02	nm?		U:
32		$(447.97, 739.48)$	17.27	1.19	-0.36	0.82	1.45	nm		U:
33		$(426.87, 751.19)$	18.94	1.11		0.67	1.41	m		
34	FM3119	$(347.72, 751.85)$	15.31	0.44	0.19	0.31	0.69	m	B9V	
34a		$(385.74, 769.61)$	19.3:			0.51	0.97	nm		
35		$(354.12, 738.94)$	17.09	0.99	-0.43	0.59	1.20	nm		U:
36		$(208.90, 762.80)$	18.29	1.64		0.79	1.59	nm		
36a		$(220.96, 752.68)$	18.66	0.72		0.47	1.01	nm?		
37	FM3118	$(295.80, 730.30)$	15.74	0.63	0.35	0.39	0.79	nm		
38	LSS39	$(368.10, 715.92)$	16.32	0.40	0.34	0.26	0.57	m		U:
39	FM4024	$(401.36, 718.58)$	13.11	1.22	1.08	0.70	1.35	nm		
40	FM4023	$(438.45, 708.31)$	14.57	0.21	-0.33	0.19	0.42	m	B3V	
41		$(504.01, 699.87)$	18.15	1.23		0.57	1.10	nm		
41a		$(542.73, 735.04)$	18.83	1.00		-0.24	1.04	m		B, V:
42		$(572.97, 712.72)$	18.48	1.47		0.74	1.48	nm		
43	MC11	$(592.96, 713.84)$	16.99	0.68		0.40	0.91	m		
44	FM4020	$(588.51, 726.19)$	14.34	1.16	1.04	0.76	1.42	nm		U:
45		$(892.35, 717.83)$	18.3:			0.59	1.33	nm		
46	FM4058	$(854.38, 691.00)$	14.57	0.50		0.32	0.67	nm		
47	MC3	$(819.77, 677.11)$	16.92	0.64		0.35	0.75	m		
48	FM4027	$(869.90, 670.20)$	15.53	0.52	0.13	0.35	0.70	m		
48a		$(446.09, 675.64)$	19.16	1.83		0.75	1.41	nm		
49	LSS37	$(377.48, 692.93)$	16.98	0.63	0.17	0.43	0.88	m		
50		$(367.03, 700.30)$	19.85	1.53		0.52	1.61	nm		B, V:
51		$(201.57, 709.31)$	19.33	2.05		1.28	2.57	nm		
52		$(184.79, 708.98)$	18.17	0.86		0.05	1.02	m		
52a		$(159.54, 710.95)$								$R = 19.1$:
53	FM3116	$(188.15, 691.38)$	16.38	0.79		0.47	0.98	nm		
53a		$(183.71, 671.96)$	19.15	1.17		0.67	1.28	nm?		
53b		$(202.32, 665.63)$	19.05	1.09		0.47	1.17	m		

TABLE 1 (CONTINUED)

Nr.	Others	(X, Y)	V	$B-V$	$U-B$	$V-R$	$V-I$	Member	SpT(Q)	Remarks
54		$(226.46, 690.18)$	17.81	0.86		0.65	1.21	m		
54a		$(211.46, 694.33)$	20.14	2.56		0.99	1.85	nm		
55	FM3117	$(265.05, 659.33)$	15.08	0.66	0.16	0.39	0.78	nm		
56	MC41	$(275.88, 661.21)$	16.99	0.47	0.36	0.32	0.72	m		
57	FM4025	$(302.70, 648.22)$	15.94	0.29	0.17	0.17	0.43	m		
58		$(349.65, 653.39)$	17.70	1.01	-1.01	0.65	1.26	nm		
59	FM4026	$(391.65, 653.47)$	15.18	0.53	0.29	0.34	0.77	nm		
59a		$(408.74, 672.32)$	18.92	0.43		0.61	1.28	nm		
60		$(551.55, 666.29)$	18.78	0.78	-3.61	0.74	1.37	nm?		$U, B, V::$
61	MC61	$(580.30, 662.18)$	17.30	0.70	-0.31	0.41	0.90	m		
62		$(617.76, 652.22)$	18.12	1.09		0.63	0.13	nm		
62a		$(654.48, 650.79)$	18.9:			0.46	0.89	nm		
62b		$(668.51, 656.15)$	19.68	0.31		0.76	1.56	nm		
63	FM4028	$(547.88, 650.05)$	14.43	0.44	0.19	0.29	0.65	nm		
63a		$(530.83, 654.35)$	19.39	-1.13		0.80	1.56	nm		$B::$
64		$(319.09, 632.99)$	18.01	0.75		0.49	0.91	m		
65		$(368.64, 629.40)$	19.13	1.07		0.71	1.66	m		$B:$
66		$(387.20, 636.33)$	20.21	0.60		1.39	2.89	nm		
66a		$(378.17, 616.90)$	19.41	0.92		0.58	1.21	m		
66b		$(403.15, 642.00)$								$R = 19.1$
67	MC47	$(294.42, 614.72)$	16.52	0.44	0.43	0.28	0.66	m		
67a		$(335.13, 614.00)$	19.22	1.29		0.64	1.35	nm		
68		$(209.48, 599.57)$	17.06	0.89	-0.70	1.17	1.28	nm		
68a		$(200.27, 590.21)$	19.84	0.50		1.90	2.05	nm		
69		$(353.10, 587.08)$	17.75	1.21		0.67	1.33	nm		
70		$(662.84, 602.36)$	18.79	0.79		0.49	1.15	nm?		
70a		$(655.37, 612.17)$								$R = 19.0:, I = 18.6:$
70b		$(681.14, 593.24)$								$R = 19.1:, I = 18.6:$
71	FM4057	$(760.40, 610.64)$	16.15	0.89	0.66	0.56	1.08	nm		
73		$(821.16, 567.47)$	17.65	0.97		0.52	1.10	nm		
74		$(682.65, 576.51)$	19.5:			0.85	1.72	m		
74a		$(670.61, 572.82)$	20.0:			0.64	1.60	m		
75		$(705.64, 559.92)$	18.19	0.77		0.43	0.89	m		
76	FM4056	$(775.30, 540.59)$	10.85	-0.03	-0.19	-0.03	0.00	nm	B9V	
77		$(756.48, 547.47)$	16.14	0.36	-0.03	0.31	0.62	m	B8V	
78		$(759.34, 519.14)$	17.07	0.59	1.47	0.45	0.83	m		$U::$
79		$(794.22, 507.00)$	16.93	2.91		0.44	0.87	nm		$B, V:$
80	FM4032	$(652.80, 542.94)$	13.95	1.03	0.67	0.62	1.22	nm		
81		$(685.35, 528.96)$	19.94	0.89		1.24	2.45	nm		$U, B, V::$
82		$(700.52, 512.20)$	19.02	2.48		0.77	1.68	nm		$U, B, V::$
82a		$(721.71, 517.43)$	19.14	1.57		0.43	0.99	nm		$U, B, V::$
83	FM4036	$(391.87, 559.76)$	14.53	0.56	0.00	0.35	0.72	nm		
84	LSS23	$(369.64, 552.71)$	16.30	0.31	0.04	0.20	0.46	m	B9V	

TABLE 1 (CONTINUED)

Nr.	Others	(X, Y)	V	$B-V$	$U-B$	$V-R$	$V-I$	Member	SpT(Q)	Remarks
85		$(364.74, 542.84)$	18.95	2.61		0.65	1.46	nm		$U, B, V::$
86		$(381.51, 527.11)$	19.80	0.57		1.23	2.17	nm		$U, B, V::$
87	FM4042	$(254.27, 543.34)$	16.14	0.41	0.34	0.27	0.65	m		
88		$(239.44, 531.45)$	18.62	0.81		0.65	1.19	m		
89		$(300.66, 517.89)$	20.01	0.89		0.99	1.84	nm		
90	FM4041	$(289.44, 506.13)$	15.65	0.38	0.13	0.25	0.58	m	B9V	
91		$(266.65, 489.54)$	18.70	0.68		0.67	1.34	nm?		
91a		$(258.62, 480.44)$								$I = 19.0:$
92		$(243.05, 473.40)$	18.24	1.14		0.70	1.48	nm		
92a		$(247.38, 484.39)$	19.7:			0.94	1.52	nm		
93		$(206.23, 462.62)$	17.76	0.77		0.56	1.24	m		
93a		$(209.27, 426.46)$	19.8:			0.98	1.83	nm		
94		$(142.82, 448.69)$	17.34	0.97		0.59	1.14	nm		
95		$(118.27, 454.60)$	18.35	1.03		0.40	0.95	nm?		
96		$(172.19, 427.06)$	19.26	2.06		1.36	2.85	nm		
97	FM4038	$(391.25, 473.25)$	15.09	0.20	-0.14	0.15	0.34	m	B7V	
97a		$(355.54, 480.14)$								$R = 18.6:, I = 18.0:$
97b		$(363.67, 492.82)$								$R = 19.1:$
98	FM4039	$(380.95, 443.77)$	15.88	0.24	-0.02	0.13	0.36	m	B9V	
98a		$(370.53, 458.35)$								$I = 18.8:$
98b		$(353.53, 462.84)$								$I = 18.7:$
99	FM4040	$(382.84, 412.23)$	16.26	0.47	0.10	0.32	0.72	m	B9V	
100	MC6	$(708.39, 466.52)$	16.46	0.67	-0.03	0.46	0.88	m		
100a		$(669.81, 459.62)$								$I = 18.2:$
101		$(872.41, 460.27)$	18.15	1.23		0.39	0.97	nm		
101a		$(766.88, 463.78)$	20.60	0.10		1.15	2.32	nm		
102		$(784.65, 427.55)$	18.38	1.05		0.46	1.03	nm?		
102a		$(809.78, 442.41)$	19.51	1.04		0.46	1.25	m		$B::$
102b		$(805.86, 429.52)$	21.00	1.0&		1.91		m	$B::$	
103		$(774.53, 410.80)$	19.99	1.70		1.16	-3.79	nm		$B, I::$
104	FM4062	$(753.13, 396.04)$	15.53	0.42	0.12	0.27	0.60	m	B9V	
105	MC43	$(860.02, 388.50)$	16.26	0.46		0.28	0.70	m		
106	MC2	$(839.46, 375.67)$	16.75	0.78	0.07	0.44	0.93	nm?		
107		$(906.03, 367.13)$								$I = 16.9:$
108		$(738.17, 381.60)$	18.27	1.12		0.65	1.26	nm		
109		$(726.24, 391.75)$	18.66	2.00		0.61	1.29	nm		
109a		$(702.16, 401.03)$	20.1:				1.91			$I = 18.4:$
110		$(638.91, 390.36)$	18.37	0.65		0.53	1.04	nm?		
110a		$(628.49, 408.94)$	20.05	1.50		0.87	1.94	nm		$U, B, V::$
110b		$(663.00, 392.20)$								$R = 19.7:$
111	MC62	$(574.43, 374.79)$	17.90	1.16		0.50	1.14	nm		
112		$(544.61, 396.19)$	17.54	1.02		0.51	1.10	nm		
112a		$(554.89, 398.63)$	19.1:			0.74	1.37	m		

TABLE 1 (CONTINUED)

Nr.	Others	(X, Y)	V	$B-V$	$U-B$	$V-R$	$V-I$	Member	SpT(Q)	Remarks
113	MC64	$(515.06, 390.25)$	17.92	1.44		0.76	1.51	nm		
114	MC63	$(503.99, 363.96)$	17.30	0.61		0.39	0.83	m		
114a		$(521.46, 366.67)$								$R = 19.3$:
115	FM4045	$(439.16, 378.50)$	12.30	0.06	-0.64	0.07	0.22	m	B2V	
115a		$(450.80, 392.63)$	18.1:			0.44	1.07	m		
115b		$(423.39, 396.54)$	19.0:			0.56	1.19	m		
116		$(402.79, 381.59)$	18.65	1.51	-1.38	0.61	1.20	nm		
117		$(200.81, 358.83)$	17.61	0.75		0.41	1.01	m		
117a		$(207.19, 368.53)$								$R = 19.1$:
118		$(170.06, 367.99)$	18.16	0.64		0.45	0.93	nm?		
119		$(175.58, 332.68)$	19.38	0.97		0.92	2.07	m		
119a		$(131.29, 332.47)$	19.11			-0.09	0.94	nm		
119b		$(200.33, 333.54)$	19.85			1.06	1.11	nm		
120		$(314.60, 327.28)$	17.19	0.79	2.65	0.45	0.93	m		U ::
120a		$(331.33, 332.68)$								$R = 20.0$:
121	FM4044	$(375.93, 325.56)$	15.49	0.24	-0.16	0.17	0.49	m	B6V	
121a		$(360.77, 352.08)$	19.9:			0.86	1.68	m		
121b		$(402.52, 339.50)$	19.7:			0.77	1.28	nm		
121c		$(412.60, 320.61)$								$R = 18.8$:
122		$(536.67, 344.29)$	17.64	1.07		0.51	1.15	nm		
123		$(519.49, 326.59)$	17.19	0.82		0.51	1.01	m		
124		$(622.24, 324.36)$	18.91	3.04		0.71	1.39	nm		U, B, V ::
124a		$(653.15, 336.00)$								$R = 19.5$:
124b		$(649.54, 368.71)$								$R = 18.6$:
124c		$(643.00, 330.10)$								$R = 19.3$:
125		$(734.10, 314.50)$	16.95	0.80		0.50	1.00	nm?		
126	FM4060	$(840.53, 340.69)$	12.30	0.21	0.02	0.11	0.30	nm	B9V	
127	FM4061	$(822.36, 333.79)$	14.96	0.56	0.16	0.34	0.72	nm		
128		$(805.40, 318.33)$	16.74	0.52		0.29	0.68	m		
128a		$(815.40, 317.26)$	19.5:			0.91	1.89	nm		
129	FM3108	$(200.19, 298.28)$	13.48	0.96	0.59	0.58	1.16	nm		
130	FM3110	$(123.34, 279.60)$	16.41	0.53	-0.08	0.40	0.89	m		
130a		$(170.32, 277.78)$	18.56	1.76	-2.17	0.80	1.70	nm		
130b		$(169.82, 278.05)$								$U = 13.8$:
130c		$(111.45, 278.19)$								$U = 12.7$:
131	FM3109	$(166.86, 258.30)$	15.54	0.48	-0.04	0.31	0.70	m		
131a		$(151.50, 246.61)$								$B = 22.4$:, $R = 19.2$:
132	FM3106	$(298.83, 305.03)$	16.23	0.51	-0.07	0.37	0.77	m		
132a	FM3107	$(263.24, 267.53)$	16.08	0.82	0.56	0.55	1.08	nm		
132b		$(289.30, 246.28)$	20.08	0.83		1.27	1.32	nm		B, V ::
132c		$(319.83, 213.97)$								$B = 19.9$:, $R = 18.5$:
132d		$(345.36, 207.17)$								$I = 18.5$:
133		$(393.29, 296.82)$	18.00	0.41		0.38	0.85	nm		

TABLE 1 (CONTINUED)

Nr.	Others	(X, Y)	V	$B-V$	$U-B$	$V-R$	$V-I$	Member	SpT(Q)	Remarks
134	FM4043	$(361.41, 286.87)$	15.19	0.67	0.14	0.41	0.93	nm		
135		$(368.10, 270.58)$	17.77	3.49	-0.35	0.44	0.92	nm		
136		$(427.02, 283.99)$	16.80	0.54	-0.28	0.64	0.79	nm		
137		$(548.69, 307.76)$	16.73	0.76	-0.14	0.50	1.00	nm?		
137a		$(539.82, 292.02)$								$B = 20.6{:}, R = 19.4{:}$
137b		$(553.74, 298.19)$								$B = 21.3{:}, R = 19.5{:}$
138		$(561.46, 289.40)$	16.67	0.55	0.47	0.68	1.16	m		
138a		$(579.00, 310.83)$	18.40							$R = 18.7{:}$
139	FM4046	$(561.99, 281.17)$	15.47	0.54	0.13	0.37	0.79	m		
140		$(685.55, 284.98)$	18.42	1.27		0.71		nm		$B{:}$
140a		$(689.55, 258.21)$								$R = 18.7{:}$
140b		$(679.36, 250.48)$								$R = 19.1{:}$
141		$(679.50, 262.50)$	18.19	1.12		0.59		nm		
141a		$(767.74, 220.61)$								$B = 19.9{:}, R = 18.1{:}$
142		$(570.94, 245.99)$	16.90	0.68		0.41	0.87	m		
143		$(523.91, 217.16)$	17.57	0.90		0.11	1.14	nm?		
143a		$(508.25, 196.28)$								$R = 18.9{:}$
144		$(583.26, 200.75)$	17.86	0.78		0.44	1.04	m		
145	FM4063	$(656.06, 200.29)$	16.18	0.73		0.47	0.98	nm		
146	FM3105	$(471.97, 175.50)$	15.47	0.21	-0.09	0.20	0.50	m	B8V	
146a		$(425.65, 167.45)$								$I = 18.1{:}$
146b		$(429.08, 180.75)$								$R = 18.4{:}, I = 19.0{:}$
147		$(617.29, 162.94)$	17.62	-0.79		0.50	0.97			
148		$(671.47, 168.80)$	16.09	0.44	0.09	0.25	0.61	m	B8V	
149		$(697.25, 168.41)$	18.57	1.62		0.58	1.34	nm		
149a		$(781.24, 164.88)$								$I = 18.6{:}$
150		$(837.75, 162.32)$	19.69	0.78		0.80	2.20	nm		$B{::}$
151		$(871.14, 161.67)$	17.27	1.00		0.62	1.34	nm		
152		$(908.17, 181.83)$								$I = 15.3{:}$
153		$(907.54, 149.32)$								$I = 17.0{:}$
154		$(896.30, 124.65)$	15.1:							
154a		$(871.54, 130.67)$								$R = 19.0{:}$
155		$(712.16, 131.30)$	18.56	1.90		0.75	1.41	nm		$U, B, V{::}$
155a		$(671.50, 110.00)$								$R = 19.8{:}$
156		$(413.77, 132.67)$	17.79	0.96		0.47	1.01	nm?		
156a		$(425.20, 167.06)$								$I = 18.1{:}$
156b		$(430.65, 180.29)$								$I = 19.0{:}$
157		$(398.46, 124.41)$	19.10	1.20		0.73	1.32	nm?		
157a		$(375.15, 132.24)$								$R = 19.5{:}$
157b		$(431.00, 104.05)$								$R = 18.4{:}$
158		$(284.08, 176.13)$	18.8:			0.77	1.39	m		
159		$(189.79, 204.04)$								$R = 19.8{:}, I = 18.5{:}$
160		$(159.05, 185.19)$								$R = 18.8{:}$

TABLE 1 (CONTINUED)

Nr.	Others	(X, Y)	V	$B-V$	$U-B$	$V-R$	$V-I$	Member	SpT(Q)	Remarks
161		$(196.14, 169.67)$								$R = 19.1:$
162		$(176.21, 144.99)$								$R = 19.5:$
1*		$(474.28, 641.30)$	18.58	1.34		0.73	1.42	nm		
2*	FM4029	$(551.85, 638.78)$	15.69	0.48	0.21	0.44	1.01	m	B9V	$B:$
3*		$(548.74, 632.24)$	16.91	1.70		1.61	3.20	nm		
4*	MC14	$(561.95, 629.73)$	16.01	0.33	-1.68	0.27	0.59	nm?		
4a*		$(572.28, 629.00)$								$R = 18.7:$
5*	FM4030	$(603.95, 621.73)$	14.92	0.40	0.07	0.26	0.59	m	B8V	
6*		$(537.57, 610.66)$	17.29	0.60	-0.08	0.41	0.88	m		
7*		$(506.23, 604.44)$	17.39	0.72	0.32	0.57	1.03	m		$U::$
7a*		$(494.24, 603.80)$								$R = 19.4:$
7b*		$(495.89, 591.20)$								$R = 19.3:$
8*		$(616.71, 617.25)$	19.20	1.93		0.46	0.91	nm		$B::, V:$
9*		$(632.44, 607.49)$	19.91	0.75		0.07	2.07	nm		$B::, V:$
10*	LSS30	$(552.40, 594.58)$	16.74	0.44	0.58	0.26	0.59	m		
10a*		$(545.36, 594.00)$								$R = 18.0:$
10b*		$(550.70, 580.50)$								$R = 19.0:$
11*	FM4031	$(615.97, 588.01)$	15.53	0.71	0.14	0.44	0.88	nm		
11a*		$(633.39, 585.11)$								$R = 19.0:$
12*	FM4033	$(586.41, 577.57)$	16.00	0.37	0.14	0.25	0.52	m	B9V	
12a*		$(593.86, 599.17)$								$R = 18.8:$
13*	FM4034	$(522.63, 571.76)$	15.69	0.50	0.16	0.35	0.76	m	B8V	
13a*		$(532.00, 564.08)$								$R = 19.9:$
14*		$(500.67, 573.13)$	19.52	0.73	-1.60	0.44	1.37	nm		$U::, V:$
15*	FM4035	$(470.55, 572.30)$	15.17	1.11	0.80	0.67	1.30	nm		
16*		$(429.89, 569.75)$	17.81	0.86		0.73	1.44	m		
17*		$(425.09, 571.83)$	18.33	0.90		0.64	1.36	m		
18*		$(552.35, 565.02)$	19.85	0.65		1.06	3.00	nm		
19*		$(610.64, 566.96)$	22.46	-2.67		2.44	3.88	nm		$V:$
20*	FM4054	$(570.29, 555.63)$	15.36	0.25	0.04	0.21	0.46	m	B9V	
21*		$(421.90, 556.06)$	19.76	1.45		1.00	1.81	nm		
22*		$(506.64, 551.79)$	20.35	0.97		1.11	2.07	nm		$B::, V:$
23*	FM4055	$(572.22, 545.48)$	14.30	0.26	-0.27	0.21	0.45	m	B5V	
24*		$(465.05, 550.41)$	18.52	0.60		0.63	1.05	nm		
25*	LSS21	$(460.32, 541.30)$	16.53	0.61	1.39	0.60	0.88	nm?		$U::$
26*		$(486.25, 544.97)$	19.23	1.19		0.16	1.11	nm?		$B::$
27*	MC68	$(482.04, 533.10)$	17.0:			0.65	1.31	m		
28*		$(511.14, 531.85)$	18.12	0.24		-1.12	1.41	nm		$B::$
29*		$(518.22, 533.52)$	18.87	0.35		-0.33	1.49	nm		$B::$
30*	LSS19	$(540.56, 531.16)$	15.52	0.32	0.11	0.23	0.53	m	B9V	
31*	FM4053	$(564.64, 531.01)$	13.10	0.19	-0.54	0.15	0.35	m	B2V	
32*		$(587.66, 534.74)$	18.58	1.09		0.79	1.61	nm?		
33*		$(587.22, 527.15)$	18.60	0.69		0.95	1.84	nm?		

TABLE 1 (CONTINUED)

Nr.	Others	(X, Y)	V	$B-V$	$U-B$	$V-R$	$V-I$	Member	SpT(Q)	Remarks
34*	MC66	(640.06, 535.57)	17.00	0.94	−1.76	0.76	1.53	nm		$U::$
35*		(634.44, 532.57)	17.18	0.75		0.56	1.08	m		$U::$
36*	FM4050	(492.79, 522.91)	12.34	0.16	−0.43	0.13	0.29	m	B3V	
37*		(508.68, 519.48)	18.06	−2.56		2.73	2.98	m		
38*		(405.03, 533.95)	18.23	0.97		0.63	1.27	m		
39*	FM4037	(418.12, 519.26)	14.50	0.17	−0.30	0.13	0.31	m	B5V	
40*		(550.53, 514.28)	18.18	0.52		0.53	1.01	nm		
41*		(509.31, 509.24)	16.02	2.12	−0.45	−1.64	−1.37	nm		
42*		(460.40, 501.71)	19.21	1.23		0.82	1.77	nm?		$B::$
43*	MC67	(577.08, 510.65)	17.66	0.65		0.49	0.88	m		
44*	LSS13	(542.91, 504.31)	14.51	0.29		0.32	0.61	m		
45*	FM4052	(535.85, 497.77)	12.81	0.19	−0.55	0.15	0.35	m	B2V	
46*	FM4051	(521.65, 503.44)	11.05	0.15	−0.64	0.15	0.33	m	B1V	exciting star
47*	LSS11	(622.00, 491.88)	16.79	0.77	−0.64	0.51	1.03	nm?		$U::$
48*		(504.13, 486.24)	17.61	0.73	−0.60	0.61	1.21	m		$U, B::$
49*	MC65	(482.08, 481.02)	17.66	0.94	−0.06	0.63	1.28	nm?		$U::$
50*		(518.72, 479.39)	18.11	−0.32	0.19	0.75	1.45	nm		$U, B::$
51*		(440.87, 475.31)	19.28	0.22		0.91	1.77	nm		
51a*		(448.91, 476.35)								$R = 19.3:$
52*	LSS9	(430.63, 463.82)	16.74	0.67	−0.04	0.39	0.84	nm?	B3V?	
53*		(468.05, 458.79)	18.40	0.34	0.24	0.49	1.08	nm		
54*	FM4049	(476.98, 451.85)	15.07	0.24	−0.21	0.14	0.36	m	B6V	
55*		(508.58, 459.47)	18.07	3.48		0.79	1.54	nm		$B::$
56*	FM4047	(550.31, 449.83)	14.52	0.29	−0.35	0.19	0.49	m	B3V	
57*		(638.77, 471.45)	18.19	1.30	−0.91	0.65	1.39	nm		$U::$
57a*		(646.41, 485.15)								$R = 19.1:$
58*	MC7	(644.95, 445.62)	16.32	0.31	0.21	0.26	0.56	m		
59*		(590.58, 471.87)	20.79	−0.00		1.24	2.51	nm		$B::$
60*		(576.67, 458.46)	19.89	0.58		0.51	1.10	nm		$B::$
61*		(589.63, 451.42)	19.13	0.67		0.58	1.28	nm		$B::$
62*	LSS5	(504.37, 434.65)	16.45	0.33	0.22	0.19	0.48	m	B8V	
63*		(411.39, 438.71)	18.28	1.57		0.76	1.72	nm		
64*	FM4048	(517.24, 425.75)	15.46	0.22	0.05	0.17	0.42	m	B9V	
65*	LSS3	(553.59, 422.77)	16.30	0.37	0.35	0.27	0.58	m		
66*		(544.66, 396.13)	17.57	2.09		0.51	1.09	nm		
67*		(628.48, 408.94)	19.92	−1.10		0.81	1.89	nm		
68*		(550.39, 397.99)	19.25	1.58		0.74	1.18	nm		
		$1\sigma =$	0.02	0.02	0.04	0.01	0.01			

NOTES TO TABLE: Stars followed by an asterisk belong to the inner region of Haffner 19 stars preceeded by "FM, LSS or MC" correspond to the designation given by FM74, Labhardt et al. (1992) or Munari & Carraro (1996), respectively.

We had problems with the offset guiding system, which presented sporadic leaps during an exposure, so we chose a full set of images consisting of the best exposed and well-guided image in each of the filters used. These were reduced with the help of the IRAF[2] utility package. The bias-, dark current-, cosmic ray- and flat field-corrected frames were then used to do aperture photometry of the program stars contained in the cluster using the QPHOT subroutine of IRAF in the Johnson/Cousins $UBV(RI)_c$ photometric system (see Figures 3 and 4 for stellar identifications and designations). The apertures were determined with the curve-of-growth method for the images in question and, since the stars were of the same size in the frames regardless of the filter used, we made the compromise of using a 5 pixel radius circle for centering, a 10 pixel radius circle for the flux measurements and an annulus with inner and outer radii of 10 and 20 pixels, respectively, for the sky estimates. The stellar images were well within the 10 pixel radius circle used for the flux determinations. We preferred to carry out manually the individual measurements. If the flux of a star in a given filter was consistent between three or more independent measurements, all of which were cleared with an 'OK' flag by the QPHOT subroutine, it was averaged to build the magnitudes and colors in the instrumental system. Only the very few objects that were too faint or too crowded, or suffered from variable background, were excluded from the final list of stars given in Table 1. Seasonal extinction coefficients were used to correct for the atmospheric extinction (Schuster 2001, private communication; see also Schuster & Parrao 2001). Subsequently, the resulting instrumental magnitudes and colors were linearly transformed to the reference systems following normal procedures (e.g., Mitchell 1960). Any systematic error due to the assumed extinction coefficients is compensated by the zero terms of the transformations from the natural to the reference system. Given the good results of the aperture photometry (see Figures 1 and 2), we did not carry out a subsequent PSF photometry since our data achieve the same quality as those obtained by other authors using the latter techique (e.g., MC96, LSS92, and references therein).

The principal problem when comparing photometric data of distinct sources is the calibration used to tie the observations to the reference sys-
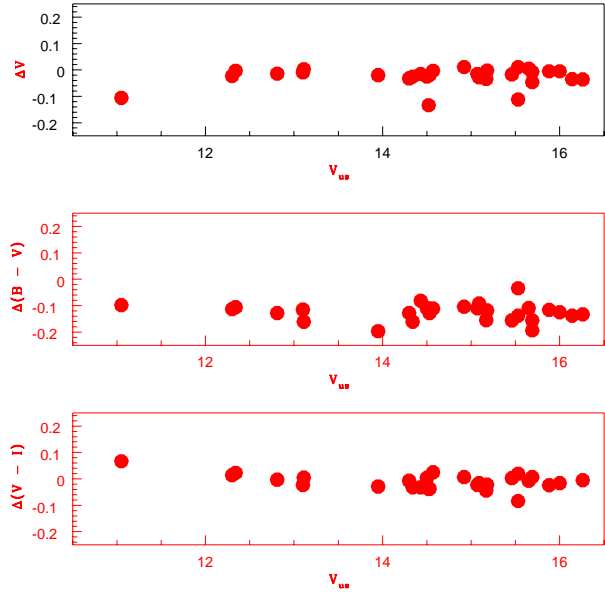
Fig. 2. The differences in magnitude and color ΔV, $\Delta(B-V)$ and $\Delta(V-I)$ between this paper (us) and MC96 versus V_{us} are displayed in the upper, middle and lower panels, respectively.

tems. Many (basically secondary) systems have proliferated in the last three decades (e.g., Lamla 1982; Taylor 1986; Moro & Munari 2000, and references therein), depending mostly on the detectors used to carry out the observations. Since this work is mainly intended to complement that of FM74 and MC96 and, since the data of these authors are directly traceable to primary UBV and VRI photometric systems, we opted to refer our observations to their systems (Johnson's UBV and Cousin's RI filters, respectively). We then proceeded to linearly tie the natural magnitudes and colors to FM74's UBV (*photoelectric*) and MC96's $V-R$, $V-I$ (*CCD-photometric*) systems with at least 22 and 29 stars in common, respectively, and following the procedure outlined by Mitchell (1960). We give the coefficients and zero terms of the transformations from the natural to the standard or reference systems in Table 2.

In Table 1 we present the resulting $UBV(RI)_c$ photometry and its expected (1σ) standard deviations for an individual star that result from the transformations of the reference stars in the instrumental system into the standard systems of FM74 and MC96. For the fainter stars, the Schottky noise terms dominate. We estimate the magnitude uncertainties as follows: with $\lambda = U, B, V, R, I$ and for $m_\lambda < 14$, the uncertainty is $\varepsilon(m_\lambda) \simeq 0.01$; for $14 < m_\lambda < 16$, $\varepsilon(m_\lambda) = 0.015$; for $16 < m_\lambda < 18$, $\varepsilon(m_\lambda) = 0.036$ and for $m_\lambda > 18$, $\varepsilon(m_\lambda) \geq 0.05$.

TABLE 2

ZERO POINTS AND TRANSFORMATION COEFFICIENTS

Color or Magnitude[a]	μ	σ_μ	z_0	σ_{z_0}	r[b]
$(U-B)_{\rm J}$	$+0.819$	0.014	-2.135	0.038	0.953
$(B-V)_{\rm J}$	$+1.092$	0.039	-1.468	0.069	0.988
$V_{\rm J}$	$+0.054$	0.029	-3.628	0.052	0.200
$(V-R)_{\rm c}$	$+0.991$	0.037	-0.211	0.021	0.994
$(V-I)_{\rm c}$	$+1.051$	0.023	$+0.216$	0.045	0.998
y	-0.014	0.004	-3.16	0.07[c]	$\cdots$
$(b-y)$	$+1.026$	0.007	$+0.76$	0.009	$\cdots$
$m1$	$+1.005$	0.016	-0.95	0.012	$\cdots$
$c1$	$+0.906$	0.012	$+1.12$	0.023	$\cdots$
β	$+1.004$	0.002	$+3.37$	0.014	$\cdots$

[a]$y = V_{\rm J}$, $m1 = (u - v) - (v - b)$ and $c1 = (v - b) - (b - y)$.

[b]We searched for a two-parameter (μ, z_0) solution with the RainBow.v01 reduction package, finding a correlation coefficient $r \geq 0.985$, except for y, where $r = 0.130$. Average seasonal atmospheric extinction coefficients were adopted: $\langle\kappa_y\rangle = 0.15$, $\langle\kappa_{b-y}\rangle = 0.049$, $\langle\kappa_{m1}\rangle = 0.047$, $\langle\kappa_{c1}\rangle = 0.11$ (cf. Schuster & Parrao 2002 and references therein).

[c]40% thin clouds over the sky.

In Fig. 1 we compare the deviations of our $(B-V)$ and $(V-I)$ indices from those by MC96 as a function of color and in Fig. 2a we compare the deviations of our V magnitude and $B-V$ and $V-I$ color indices from those of MC96 as a function of the magnitude. From the figures, it is evident that our photometry is comparable in quality to that of MC96 (or LSS92, see MC96). MC96's and our photometric systems transform linearly and reasonably well, with few exceptions: only four stars in common for which the magnitude differences between any two given systems (i.e., this paper versus MC96 and MC96 versus LSS92) deviate by more than the 2σ given by the linear regressions (stars FM4047, FM4051, FM4055, and MC14). MC14 is a very reddened star (see star 4* of Table 1) and we suspect that FM4051 (the principal exciting star of the Strömgren sphere encircling Haffner 19) is a double (see below). In conclusion, the quality of the photometric systems are equivalent and there are no significant magnitude or color-dependent deviations between MC96 or LSS92. The systematic deviation in the $(B-V)$ color between FM74 (used in this paper) and MC96 has already been discussed by the latter.

Figures 3 and 4 are I-band images of the outer and inner regions of Haffner 19, respectively, and are shown for identification purposes of the stars. Like the other exposures analyzed here, Fig. 3 has a field
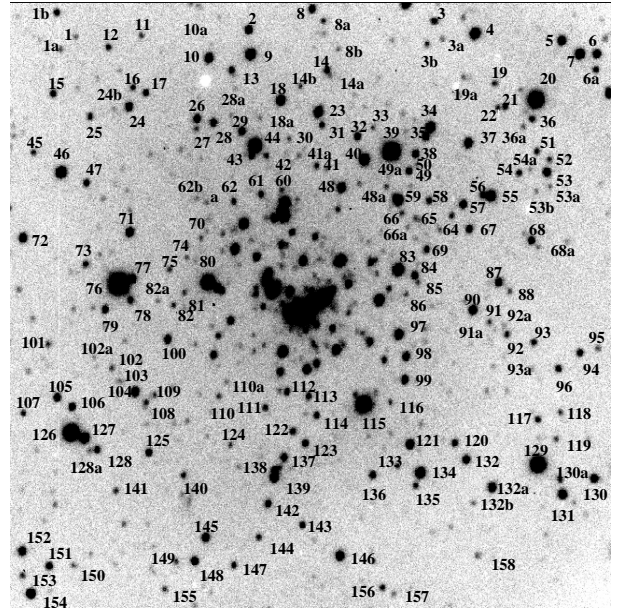
Fig. 3. Map of the exterior region of Haffner 19 in the I filter. North is at the top, east to the left. The image size is $\approx 3.2 \times 3.2$ arcmin^2.

of view of 3.2×3.2 arcmin^2 with star CD$-25°5202$ near its center. It covers more than the size of the cluster ($\phi_{\rm fwhm} \simeq 1.'2$, FM74) or the size of the Strömgren sphere ($\phi \simeq 2.'0$, see below, this work).
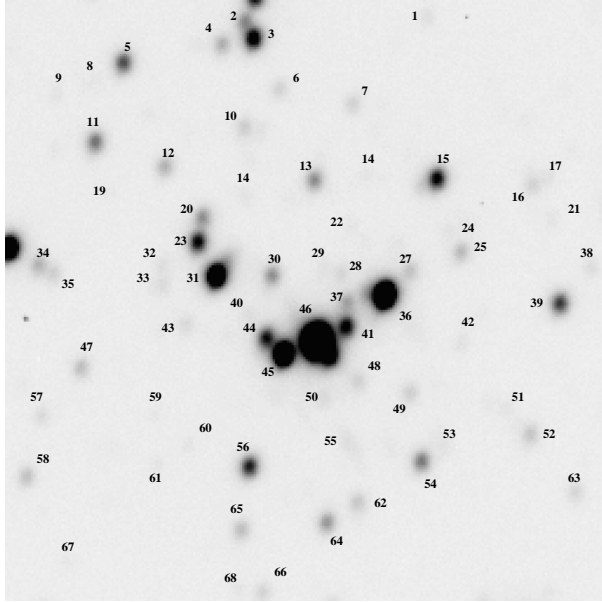
Fig. 4. Map of the interior region of Haffner 19 in the I filter. North is at the top, east to the left. Image size is 1.2×1.2 arcmin^2.

In Table 1 we present the results of the broadband $UBV(RI)_c$ photometry of the program stars (cf. Figs. 3 and 4). To differentiate between the two sets of numbers used here, stars enumerated in Fig. 4 are distinguished from the other stars of Fig. 3 by appending an asterisk to their designation number; the former correspond to the inner region of the cluster. This inner region was chosen to approximately contain Haffner 19, as given by FM74 and the Strömgren sphere reported here (see also PM76). In the second column we give an alternative designation of the principal objects studied here. Columns 3 and 4 are the X and Y positions on the original CCD frame. Columns 5 to 9 correspond to the visual magnitude V and the color indices $B-V$, $U-B$, $V-R$, and $V-I$, respectively. In column 10 we give a membership qualifier to the cluster: m = member or most probably a member, nm = non-member, and nm? = non-member with doubts. In column 11 we give the MK spectral type of the star following the Q-method (Johnson & Morgan 1953) and, finally, in column 12 we give additional comments regarding the star and its photometric data. In total, we present photometric data of 334 stars (249 in B and V). Our sample is complete down to $m_\lambda = 19$ ($\lambda = U, B, V, R, I$).

2.2. uvbyβ Photometry

Strömgren/Crawford or $uvby\beta$ photometry is important in determining the principal parameters of

Haffner 19, since it allows us to test, with independent calibrations, results obtained with broadband photometry. On the night of 2000 February 27 (UT) we had the opportunity to observe six stars of the Haffner 19 region in the $uvby\beta$ photoelectric system, using the 1.5 m "Harold L. Johnson" telescope and the Danish six channel photometer of SPMO. For details of this last instrument consult Nissen (1984). The weather was fair with variable high thin clouds. It is our experience, and also that of others (Grønbech, Olsen, Strömgren 1976; Olsen 1983; Schuster & Nissen 1988), that, under such observing conditions, poor magnitude estimates (error $\leq 10\%$, cloud cast dependent) but good color determinations (error $< 1\%$) are obtained. (One measures the different channels simultaneously, which are affected by grey extinction of the clouds in the same way.) This is corroborated by the estimated errors given by the transformations to the standard system of the observed reference stars (cf. Tables 2 and 3). The sky was usually measured 30 arcsec in right ascension from the object, and a 14 arcsec diameter diaphragm was used for the observations. Care was taken to exclude unwanted stars. We had an airmass $X \geq 2$ during the observations of the region, given basically by the geographic site of the observatory. A dozen standard stars were observed during the night to tie the observations to the Strömgren (1966)/Crawford (1979)/Olsen (1984) photometric systems with yellow/white-blue/red reference stars, respectively. The transformation matrix of the night is in good agreement with the mean matrix for the observing run of the main program, to be discussed elsewhere. The reductions were carried out with the Rainbow.v01 photoelectric reduction package following Mitchell (1960, see also Chavarría, de Lara, & Chavarría-K. 2001). The resulting photometry and the uncertainty in a single observation (1σ per unity air mass), estimated from the observation and transformation of the standard stars to the reference system, are given in Table 3.

3. RESULTS AND DISCUSSION

3.1. CCD Photometry

With the photometric data of Table 1, the interstellar reddening and distance to the cluster can be estimated in several ways: (i) by making a visual adjustment of the zero age main sequence (ZAMS) given by Schmidt-Kaler (1982) to the data in the magnitude-color diagram (basically, the shift of the steep bluer section of the ZAMS in the $B-V$ axis gives E_{B-V} and the shift of the inflection of the slope of the ZAMS curve around spectral type A0 stars

TABLE 3

$uvby\beta$ PHOTOMETRY OF SELECTED STARS IN HAFFNER 19 [a]

Nr.	$b-y$	β	m1	c1	AIR	J.D.
36*	0.18	2.58	0.06	0.19	2.05	51601.7747
39*	0.77	2.48	0.65	0.93	2.29	51601.7983
46*	0.24	2.63	−0.02	0.17	1.99	51601.7649
76	−0.01	2.86	0.18	0.97	2.02	51601.7701
115	0.17	2.56	−0.01	0.19	2.15	51601.7865
126	0.15	2.77	0.21	0.86	2.10	51601.7806
$1\sigma =$	0.01	0.01	0.01	0.02	$\cdots$	$\cdots$

[a]With the exception of Julian date, all table entries were rounded from three to two decimals.

in the magnitude axis fixes the apparent distance modulus, cf. Figure 5); (ii) from the spectral types, intrinsic colors and absolute magnitudes of cluster stars given in the literature (i.e., the intrinsically brightest and bluest ones); and, finally, (iii) using the Q-method of Johnson & Morgan (1953) and following procedure (ii). Note that the brighter cluster stars clearly depict a main sequence in the color-magnitude or $(V, B-V)$ diagram (cf. Fig. 5), an indication that the hotter members of Haffner 19 are indeed main sequence stars.

In the first case, the color excess E_{B-V} was found to be 0.41 ± 0.01 and the apparent distance modulus, 15.2 ± 0.1. Adopting a total-to-selective extinction ratio of $A_V/E_{B-V} = 3.3$, calculated for the case of early spectral-type stars with the relation

$$A_V/E_{B-V} = 3.30 + 0.28\,(B-V)_0 + 0.04\,E_{B-V}, \quad (1)$$

(cf. Schmidt-Kaler 1982), we obtain a true distance modulus of $5\log d - 5 = 13.8\pm0.1$ or $d = 5.8\pm0.1$ kpc.

In the second case, for the 5 cluster stars with spectral types determined spectroscopically (cf. Lodén 1965, FM74, MC96), and assuming luminosity class V for the stars, the intrinsic colors for the ZAMS stars given by Schmidt-Kaler (1982) and the photometry of Table 1, we found a mean color excess $E_{B-V} = 0.39 \pm 0.03$, a mean distance modulus of $5\log d - 5 = 13.62 \pm 0.07$ and a distance of $d = 5.3 \pm 0.2$ kpc. We also found a quotient $E_{U-B}/E_{B-V} = 0.64 \pm 0.08$ for these 5 stars. This value, although smaller than the canonical value of 0.72 (e.g., Mathis 1990), is in reasonable agreement with this given the error spread observed.

Finally, for the third case, if we consider a nor-

mal extinction law for the region (MC96, this work), we can determine photometrically the MK spectral types of the program stars (early B to early A) with the Q-index given by the photometry and its calibrations with the MK spectral types by Johnson & Morgan (1953), for which the following expression holds

$$Q = (U-B) - (B-V)\left(\frac{E_{U-B}}{E_{B-V}}\right). \quad (2)$$

In our case, we assumed the canonical value for the mean interstellar (IS) extinction law, $E_{U-B}/E_{B-V} = 0.72$. According to Johnson & Morgan (1953), the method works for stars with spectral types within the range of B0 to A0, with an expected uncertainty of one spectral subclass. We adopted luminosity class V for the bluer program stars. The method allowed us to assign MK spectral types to the 33 brightest stars and they are reported in column 9 of Table 1. With the spectral types that resulted from the Q-method and their corresponding ZAMS absolute magnitude M_v and intrinsic colors given by Schmidt-Kaler (1982), we determined a mean value for the distance of 5.0 ± 0.3 kpc for 29 stars of the inner and outer regions of the cluster. Stars 52* 62*, 126, and 76 were excluded in the present analysis because their distance estimates differed from the average significantly more than the scatter observed for the rest of the program stars. Except for star 62*, the other 3 are non members of the association (see next section). The color excess was found to be 0.44 ± 0.03.

It is worthwhile to mention here that, when comparing our spectral types resulting from the Q-method with those spectroscopically determined by

TABLE 4

$uvby\beta$ PHOTOMETRIC RESULTS

Nr.	SpT($[u-b]$)	SpT(β)	adopted	E_{B-V}	$V_\circ$	$5\log d - 5$	d[kpc]
36*	B2.5	$\cdots$ [a]	B2	0.41	11.0	13.4	4.8
39*	>G9[b]	$\cdots$ [a]	K5	~ 0.15	14.0	6.6	0.2
46*	B1.5	B1.5	B1.5	0.51	9.4	12.2	2.8
76	A0	A1	A1	0.0	10.8	9.9	1.0
115	B1.5	$\cdots$ [a]	B1.5	0.39	11.0	13.8	5.8
126	A0	B9.5	A0	0.24	11.6	10.9	1.5

[a]Very early type or filled in with emission or contaminated by the H II region.

[b]'>' indicates 'later than'.
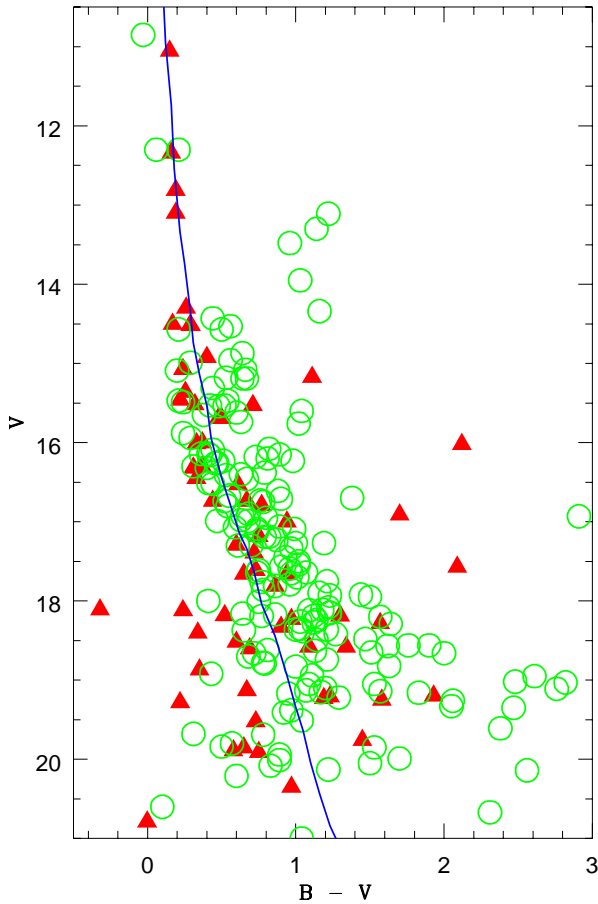
Fig. 5. Magnitude-color diagram V, ($B-V$) of Haffner 19. Triangles depict the location in the diagram of the inner region stars, while the open circles represent the location of the outer region stars. The solid line represents the ZAMS reddened with $E_{B-V} = 0.42$ and at a distance of 5.3 kpc.

MC96 (stars 34, 50, 53, 57, and 60 in their designation), we find a coincidence for two cases (stars 45* and 115 in our designation); for another two stars our resulting spectral types are earlier (23* and 31*), and for the remaining star (46*) we find a later spectral type. The deviations in spectral types fall, on average, within the expected uncertainty of ± 1 subclass.

From the color-magnitude or (V, $B-V$) diagram (cf. Fig. 5) we see that our data well fit the MS throughout a nine magnitude interval. The presence of at least 15 early B-type stars in the cluster confirms the very young nature of this conglomerate. We see from the loci of the cooler and hence redder program stars in Fig. 5 a large dispersion about the MS line (more than that in the equivalent diagram of MC96). This is because our exposures are deeper in all bands than those of MC96 and hence enable us to observe later spectral type stars (pre-main sequence, foreground and background objects, i.e., above and below the ZAMS). One also readily notes from the lower end of Fig. 5 that stars from the external region of Haffner 19 occupy more frequently the region above and to the right of the MS. If the scatter observed is partially due to the presence of PMS stars (starting at spectral type A stars), we can give an age estimate of the cluster.

3.1.1. The Program Stars, the Membership and the Reddening to the Cluster

The cluster membership of the sample stars was determined from their locations in the magnitude-color diagrams (V, $B-V$) and (I, $R-I$), and in the color-color diagrams ($U-B$, $B-V$) and ($V-R$, $V-I$), allowing for a dispersion from the MS not larger than $\Delta V = 0.3$, as given by nearby clusters such as

TABLE 5

FABRY-PEROT INTERFEROMETRIC RESULTS

Region	Points	v_r km s^{-1}	v_{lsr} km s^{-1}	d_{kin} kpc
Haffner 19	74	67.6 ± 0.10	49.80 ± 0.10	4.4 ± 0.1
Haffner 18ab	65	76.1 ± 0.12	58.30 ± 0.12	5.3 ± 0.2
NGC 2467	486	67.8 ± 0.07	50.00 ± 0.07	4.4 ± 0.1
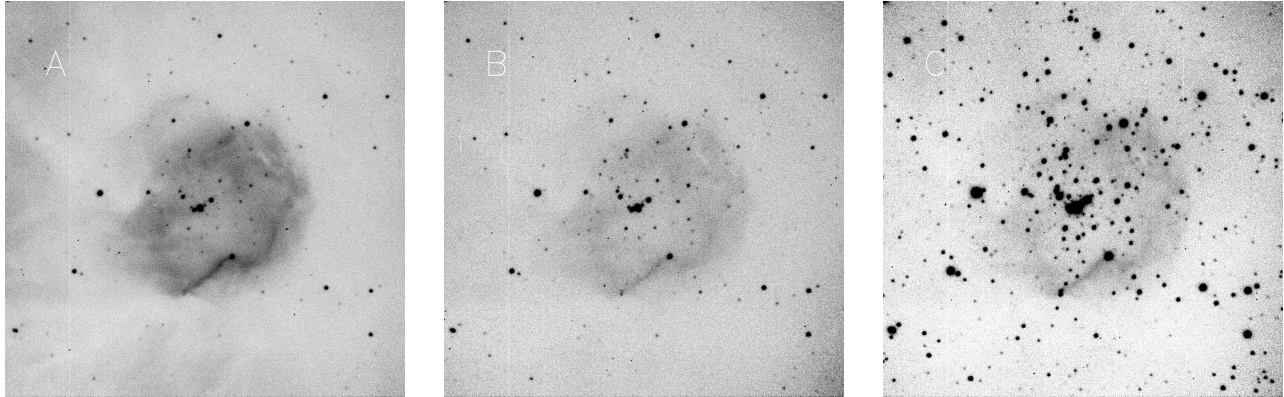
Fig. 6. Images of the Strömgren sphere around Haffner 19 taken with the 1.5 m telescope at (a) Hα; (b) [N II] λ 6583 Å; and (c) [S II] $\lambda\lambda$ 6719/6731 Å. Image size is 3.9×3.9 arcmin^2. North is at the top and east to the left.

the Pleiades, Hyades, or Praesepe, and allowing only for deviations smaller than 0.27 mag from the main linear two-color relations given by the program stars. Except for the (V, $B-V$) diagram of Fig. 5, we do not show the other diagrams, but all the necessary data are summarized in Table 1. Concluding, we find that 101 stars are cluster members (m), 27 could be members (nm?) and 132 are non-members (nm). We did not have enough information for the remaining 74 stars, or the available data were unreliable. The brightest star of the cluster, CD$-25°5202$ (= 46* in our designation), is discussed in more detail below. From the ($U-B$, $B-V$) diagram, but principally from the E_{B-V} color excesses and the spatial distribution of the 29 B-stars in the cluster, we note that the visual extinction of the cluster is moderate and fairly homogeneous around the average value of $E_{B-V} = 0.44$ and that the intercluster reddening varies by $\delta E_{B-V} \simeq 0.2$ or less. This argues against shifting the stars in a color-magnitude diagram supposing variable extinction.

3.1.2. *Regarding the Exciting Star of Haffner 19*

Star 46* of our list (CD$-25°5202$, FM4051, MC60, and LSS14) deserves special attention, since it is located in the center of Haffner 19 and is the brightest and hence most energetic object of the cluster, making it capable of producing the spherical ionized structure that surrounds it, to be discussed in more detail in § 3.3. The star was spectroscopically classified as B1.5V by W. W. Morgan (cf. Lodén 1965), B0V by FM74, B1.5 from the $uvby\beta$ photometry (see below) and B1V from the Q-method here. When plotted on an apparent modulus vs. reddening diagram, i.e., a ($V - M_V$, E_{B-V}) diagram, together with the other stars with photometric MK spectral types, its position in the diagram lies significantly below the average trend of the rest of the stars. We can identify three possible explanations for this: either the star is intrinsically brighter for its given spectral type (it could be a binary system or be hotter than its assigned spectral class), or it is nearer to the observer. In the case of a double system considered as a single star, its distance could be underestimated by as much as 40%. On the other hand, the star seems shifted to the right of the ZAMS by about $\Delta(B-V) = 0.01$ (see Fig. 5). This deviation is within the photometric errors. However, if real and due to evolution in its structure, the stellar age would then be $\approx 3.7 \times 10^6$ yr. This value is model-dependent, but one expects an age dispersion of less than about 10% because of this (cf. Claret

& Giménez 1992; Schaller et al. 1992; Schaerer et al. 1993). Since the blue members have not significantly evolved from the main sequence, metallicity plays a secondary role in their colors because the stars are too hot to be affected by metals. A reasonable assumption would be a solar-like value. On the other hand, if this (nuclear) upper limit for the age is correct, then one should explain the existence and size of the Strömgren sphere surrounding the star (see Figure 6) and the presence of pre-main sequence stars with $M_* \approx 3M_\odot$ (see below). Finally, it is interesting to note that the β-index (see next section) is too high for its spectral type, an indication that the star could be losing mass at a significant rate (i.e., P Cygni profiles of the lower Balmer lines), a characteristic found frequently in very young objects. Spectroscopic observations of the Balmer lines with medium-high dispersion could be rewarding.

3.2. *uvbyβ Photometry*

From a quick inspection of the *uvbyβ* photometry of Table 3 one readily finds that the stars are early (A to early B stars), except for star 39* which is a foreground K star with Hβ probably in emission. A more detailed analysis of the data, using the $[u-b]$ and β reddening-free indices (cf. Chavarría-K. et al. 1988 for a preliminary calibration of the former index), shows that stars 39*, 76, and 126 are foreground stars of spectral types ∼K5, A1 and A0, respectively, while stars 36*, 46*, and 115 are early B stars, in agreement with the broad band photometry. The absolute magnitudes, β indices, spectral types and temperature calibrations of Schmidt-Kaler (1982), as well as intrinsic colors from model atmospheres by Lester, Gray, & Kurucz (1986) were used here to derive the principal parameters of Table 4. Since our magnitude estimates were affected by thin high clouds (expected V uncertainty ≤ 10%, see Table 2), we preferred to adopt the visual magnitudes of the CCD (broad-band) photometry of Table 1, and together with the (photometric) spectral types of Table 4, one obtains, with $A_V/E_{B-V} = 3.3$, the unreddened visual magnitudes $V_\circ$, the distance moduli $5 \log d - 5$, and hence distances d to the objects (columns 7, 8, and 9 of Table 4, respectively). The three blue stars give a mean distance $d = 4.5\pm1.0$ kpc and a reddening $E_{B-V} = 0.44\pm0.05$. The large error bar in d is because star 46* is too bright for its spectral type B1.5V given by the *uvbyβ* photometry here and Lodén (1965). If star 46* is a binary, then the distance is larger and the dispersion in the distance from the mean becomes

smaller. In the case that star 46* consists of two B1.5V stars (the deviation of 46* from the main trend in the ΔV, $B-V$ diagram is in accordance with this), then the distance given by the three blue stars is $d = 4.8 \pm 0.7$ kpc. On the other hand, if we assume that star 46* is of spectral type B0V as given by FM74, we find a mean distance for the region, given by the three hottest stars of Table 4, of $d = 5.1 \pm 0.4$ pc. Assuming the average of the three values above we obtain $d = 4.8 \pm 0.3$ kpc and the reddening remains unchanged.

In conclusion, averaging the four distance estimates given by the broad band (3) and the intermediate band (1) photometry we obtain a true distance modulus of 13.6 ± 0.2, a mean distance of 5.2 ± 0.4 kpc, and a reddening of $E_{B-V} = 0.42\pm0.01$, which we consider the best mean values of the principal parameters of Haffner 19.

3.3. *Hα, [N II] and [S II] Imagery of Haffner 19*

A reasonably spherical gaseous structure of radius $\simeq 1''.1$, ionization bounded to the south, density bounded elsewhere and with CD$-25°5202$ in its center, is revealed in our narrow-band (3 minute exposure) images of Haffner 19. The central wavelengths of the filters are at Hα $\lambda 6583$ Å, [N II] $\lambda 6583$ Å and [S II] $\lambda 6725$ Å, taken with the 1.5 m "Harold L. Johnson" telescope of SPMO. The Hα and [N II] filters have a spectral window of $\Delta\lambda = 10$ Å, whereas that of [S II] is of $\Delta\lambda = 80$ Å (it includes 6718 and 6729 Å). The images confirm the Hα-bright knot reported earlier by PM76. Fig 6 shows the Strömgren sphere surrounding CD$-25°5202$ at the different wavelengths.

We can roughly estimate the ionization structure, size and age of the Strömgren sphere by assuming that its exciting star is of spectral type B0V, with an ionizing photon flux of $N_{\mathrm{Lyc}} = 6.6\times10^{47}$ photons s^{-1} (Felli et al. 1978) with the expressions

$$N_{\mathrm{Lyc}} = \frac{4\pi}{3} n_e^2 \alpha_{\mathrm{H}}(T) R_i^3, \qquad (3)$$

and

$$\alpha_{\mathrm{H}}(T) = 2.07 \times 10^{-11} T^{-0.5}\phi \ \mathrm{cm^3 \ s^{-1}}, \qquad (4)$$

where ϕ depends little on the temperature and $\alpha_{\mathrm{H}}(T)$ is the total recombination coefficient of hydrogen. Further assuming that the sphere is immersed in a typically homogeneous medium of density $n_e = n_p = 60$ cm^{-3} and in a stationary state with its surroundings, we have that $\alpha_{\mathrm{H}} = 3.3 \times 10^{-13}$ cm^{-3} s^{-1}

(Osterbrock 1974). From this and the two equations above we obtain:

$$R_{\rm i} = \left(\frac{3N_{\rm Lyc}}{4\pi n_{\rm e}^2 \alpha_{\rm H}} \right)^{1/3}, \qquad (5)$$

or $R_{\rm i} = 5.0 \times 10^{18}$ cm (= 1.64 pc).

With $d = 5.2$ kpc from our photometry we can derive the angular radius mentioned above for the Strömgren sphere and, assuming that it is excited solely by the B0V star, we find $\theta = R_{\rm i}/d = 1.1$ arcmin, which is in reasonable agreement with the observed value. (There are also other blue stars in Haffner 19 that contribute to the ionization of the Strömgren sphere.) We can estimate the mass contained within this Strömgren sphere $(= 4/3\pi R_{\rm i}^3 n_{\rm e} m_{\rm H})$, which is $17 M_\odot$, or about 10% of the total (gaseous + stellar) mass within it.

Finally, we can estimate an age for the Strömgren sphere since we know that, in typical H II regions, the ionization front in a molecular cloud moves with a typical velocity of $v_{\rm i} \sim 2$ km s^{-1} (e.g., Moreno-Corral et al. 1993). Given the radius of the sphere, one obtains $t = R_{\rm i}/v_{\rm i} = 8.2 \times 10^5$ yr. In conclusion, from the observations we see that star CD-25°5202 is a very young star and is principally responsible for the Strömgren sphere observed in Hα, [N II], and [S II]. The presence of the Strömgren sphere also gives additional evidence in favour of the youth of the stellar cluster.

3.4. *The Kinematic Distance.*

Using Fabry-Perot interferometric techniques, Georgelin & Georgelin (1970) estimated a kinematic distance to the adjacent H II region NGC 2467 of 3.8 kpc, based upon the measurement of radial velocities at 22 different points. With the same technique, but measuring a total of 635 points that included NGC 2467, Haffner 18ab and Haffner 19, PM76 derived a kinematic distance for the complex of 4.2 kpc. Since there are controversies regarding the physical association of the three regions that compose the complex, and since the rotational model for the Galaxy has suffered modifications (e.g., Fich, Blitz, & Stark 1989, and references therein), we have reviewed the original data and interferograms of PM76, attempting to separate each of the three regions, NGC 2467, Haffner 18ab and Haffner 19. We determined the radial velocity fields of the three regions and their respective average velocities (heliocentric and in the Local Standard of Rest), as well as the number of points measured in each region. We followed the reduction procedures outlined

by Courtès (1972, and references therein). The heliocentric radial velocities were transformed to the Local Standard of Rest in the usual way, assuming that the Sun moves at 19.5 km s^{-1} in direction $\alpha_{1950} = 18^{\rm h}01^{\rm m}00^{\rm s}$, $\delta_{1950} = 13°00'00''$. With the average radial velocities in the Local Standard of Rest of the regions, and using the Galactic constants R_0 and Θ_0 recommended by the IAU, together with the analytical model for the rotation of the Galaxy by Fich et al. (1989), we obtained the kinematic distances to Haffner 19, Haffner 18ab and NGC 2467. Our results are summarized in Table 5. Note that the resulting kinematic distances of Haffner 19 and NGC 2467 are practically the same and very similar to that obtained for NGC 2467 by PM76, whereas that of Haffner 18ab clearly differs from the two others. The latter is more distant than the former two by about 20%, or one kiloparsec. In the case of Haffner 19, although the difference between the results of the photometric and kinematic methods for the distances diminishes, it is still comparable to such (large) differences observed in other H II regions in that Galaxy quadrant.

4. FINAL REMARKS AND CONCLUSIONS.

From the photometry of 334 stars we find that the cluster consists of at least one hundred stars. The $UBV(RI)_{\rm c}$ photometry reported here does not show the presence of a high or significantly variable extinction in the direction of the cluster or within it. A mean $E_{B-V} = 0.42 \pm 0.01$ was obtained from four different methods. The photometry further shows that a normal extinction law is suitable for the region. We have confirmed the youth of Haffner 19 and we present evidence that its associated H II region is a Strömgren sphere around CD-25°5202, with an age of about 8.2×10^5 yr. With the additional time that a $15 M_\odot$ star requires to reach the ZAMS, the lower bound for the age of the complex is about 10^6 yr. From the presence of $3 M_\odot$ pre-main sequence stars, we expect an age of 2×10^6 yr, with an age dispersion given by the time a sound wave requires to traverse the complex of about 10^6 yr, assuming that the complex encircles about $120 M_\odot$ (stellar masses + ionized gas) and that it originally had a typical average molecular cloud temperature. On the other hand, if the (marginally present) deviation from the ZAMS of the brightest star of the cluster, CD-25°5202, is due to evolutionary effects of its stellar structure, then we expect an upper bound to the age of about 3.7×10^6 yr (model-dependent), regardless of the metallicity of the star. In this case, one must explain the existence of its Strömgren sphere

and the presence of A0-like pre-main sequence stars. We estimated the distance to the cluster by five different procedures (the smallest estimate was 4.4 kpc and the largest 5.8 kpc). The photometry delivers a mean distance of $d = 5.2 \pm 0.4$ kpc, which we regard as the best value for the cluster distance. We also give radial velocities and kinematic distances of Haffner 19, Haffner 18ab, and NGC 2467. The kinematic results indicate that Haffner 19 and NGC 2467 could be physically associated, but that Haffner 18ab is an independent entity and more distant than the former two.

REFERENCES

Chavarría, A., de Lara, E., & Chavarría-K., C. 2001, User's Manual of the RainBow.v01 Photoelectric Reduction Package (San Diego, CA: Instituto de Astronomía)

Chavarría-K., C, de Lara, E., Finkenzeller, U., Mendoza, E. E., & Ocegueda, J. 1988, A&A, 197, 151

Claret, A., & Giménez, A. 1992, A&A, 96, 255

Crawford, D. L. 1979, AJ, 84, 1858

Courtès, G. 1972 in Vistas Astr., ed. A. Beer (Oxford: Pergamon Press), 81

Felli, M., Tofani, G., Harten, R. H., & Panagia, N. 1978, A&A, 69, 199

Fich, M., Blitz, L., & Stark, A. A. 1989, ApJ, 342, 272

FitzGerald, M. P., & Moffat, A. F. J. 1974, AJ, 79, 873 (FM74)

_____. 1976, A&A, 50, 149

Georgelin, Y. P., & Georgelin, Y. M. 1970, A&A, 6, 347

Grønbech, B., Olsen, E. H., & Strömgren, B. 1976, A&AS, 26, 155

Haffner, H. 1957, Zs.Ap, 43, 89

Johnson, H. L., & Morgan, W. W. 1953, ApJ, 117, 313

Labhardt, L., Spaenhauer, A., & Schwengeler, H. 1992, A&A, 265, 869 (LSS92)

Lamla, E. 1982, In Landolt-Börnstein New Series, Group VI, vol. 2b, eds. K. Schaifers & H. H. Voigt (Berlin: Springer Verlag)

Lester, J. B, Gray, R. D., & Kurucz, R. L. 1986, ApJS, 61, 509

Lodén, L. O. 1965, ApJ, 141, 668

Mathis, J. S. 1990, ARA&A, 28, 37

Mitchell, R. 1960, ApJ, 132, 68

Moreno-Corral, M. A., Chavarría-K., C., de Lara, E., & Wagner, S. 1993, A&A, 273, 619

Moro, D., & Munari, U. 2000, A&AS, 147, 629

Moitinho, A. 2000, Ph.D. thesis, Instituto de Astrofísica de Andalucía, Spain

_____. 2001, A&A, 370, 436

Munari, U., & Carraro, G. 1996, MNRAS, 283, 905 (MC96)

Nissen, P. 1984, User's Manual of the Danish $uvby\beta$ Photometer (San Diego, CA: Observatorio Astronómico Nacional)

Olsen, E. H. 1983, A&AS, 54, 55

_____. 1984, A&AS, 57, 443

Osterbrock, D. E. 1974, Astrophysics of Gaseous Nebulae (San Francisco: W. H. Freeman)

Pişmiş, P., & Moreno, M. A. 1976, RevMexAA, 1, 373 (PM76)

Schaerer, D., Charbonnel, C., Meynet, G., Maeder, A., & Schaller, G. 1993, A&AS, 102, 339

Schaller, G., Schaerer, D., Meynet, G., & Maeder, A. 1992, A&A, 96, 269

Schmidt-Kaler, Th. 1982, In Landolt-Börnstein New Series, Group VI, vol. 2b, eds. K. Schaifers & H. H. Voigt (Berlin: Springer Verlag)

Schuster, W., & Nissen, P. E. 1988, A&AS, 73, 227

Schuster, W., & Parrao, L. 2001, RevMexAA, 37, 187

Strömgren, B. 1966, ARA&A, 4, 433

Taylor, B. J. 1986, ApJS, 60, 577

Carlos Chavarría-K, Estela de Lara, and Marco A. Moreno-Corral: Instituto de Astronomía, UNAM, Carretera Tijuana-Ensenada km 103, 22860 Ensenada B. C., México (mam@astrosen.unam.mx).